Available online at www.sciencedirect.com
ScienceDirect
Trans. Nonferrous Met. Soc. China 24(2014) 1969−1977
Transactions of Nonferrous Metals Society of China
www.tnmsc.cn

Effect of Schiff base as corrosion inhibitor on AZ31 magnesium alloy in hydrochloric acid solution

S. THIRUGNANASELVI[1], S. KUTTIRANI[2], Amali Roseline EMELDA[1]

1. Department of Chemistry, Sri Ramanujar Engineering College, Chennai 600048, India;
2. Department of Chemistry, BS Abdur Rahman University, Chennai 600048, India

Received 24 September 2013; accepted 3 December 2013

Abstract: Schiff base derived from the condensation reaction of analar grade 1-amino-2-naphthol 4-sulphonic acid with cinnamaldehyde was prepared under microwave condition. The Schiff base was analysed by infrared spectroscopy. This Schiff base as a corrosion inhibitor of AZ31 magnesium alloy in 0.05 mol/L HCl solution was studied. The inhibition effect of the Schiff base compound (4Z)-4-(3-phenyl allylidene amino)-3-hydroxy naphthalene-1-sulfonic acid (AC) on AZ31 magnesium alloy corrosion was studied using mass loss, potentiodynamic polarization technique, electrochemical impedance spectroscopy methods. The potentiodynamic polarization curve shows that Schiff base AC inhibits both anodic and cathodic reactions at all concentration, which indicates it is a mixed type inhibitor. EIS results indicate that as the additive concentration is increased, the polarization resistance increases whereas double-layer capacitance decreases. The adsorption of AC on the AZ31 magnesium alloy surface in 0.05 mol/L HCl obeys the Langmuir adsorption isotherm.

Key words: Schiff base; AZ31 magnesium alloy; corrosion inhibitor; potentiodynamic polarization; electrochemical impedance spectroscopy

1 Introduction

Magnesium alloy is one of the lightest metallic alloys currently used, because of its low density (1.74 gm/cm^3) and high mechanical stiffness [1]. However, the mechanical benefits of magnesium are contrasted by a high corrosion rate as compared to aluminium or steel. Because of electrochemical potential of magnesium, as illustrated in galvanic series, it corrodes easily in the presence of sea water. The high corrosion property has relegated the alloy to be used in areas unexposed to the atmosphere, including car seat electronic boxes and structural members. The demands for the use of magnesium alloys, as structural materials in automobile industry, electronic products, vibrating plates of vibrating test machines and automotive wheels, have increased in recent years [2]. Consequently, this investigation relates to the field of corrosion inhibition of magnesium alloys, since the magnesium alloys are highly prone to corrosion.

Compounds containing an azomethine group (—C═N—) are known as Schiff bases. They are usually formed by the condensation of primary amine with carbonyl compounds [3] according to the reaction as follows:

$$R—NH_2+R—COH \rightarrow R—N═CH—R+H_2O \quad (1)$$

where R may be an aliphatic or aromatic group. The Schiff bases of aromatic aldehydes with an effective conjugated system are more stable [4].

The efficiency of an organic inhibitor on metallic corrosion does not only depend on the structural characteristics of the inhibitor but also on the nature of the metal and environment. The selection of suitable inhibitor for particular system is the difficult task because of the selectivity of the inhibitors and the wide variety of environments

The choice of the inhibitor is based on two considerations, firstly the economic consideration, and secondly, it should contain the electron cloud on the aromatic ring or the electronegative atoms such as N, O in the relatively long chain compounds [5].

One of the most vital processes in the field of prevention of corrosion and its control is the use of organic inhibitors. The crucial part in the mechanistic

Corresponding author: S. KUTTIRANI; E-mail: skrani@bsauniv.ac.in
DOI: 10.1016/S1003-6326(14)63278-7

aspect of such inhibitors is the specific interaction between certain functionalities in the inhibitors with the corrosion active centres on the metal surface. Heteroatoms such as nitrogen, oxygen, and sulphur present in the inhibitors play a leading role in this interaction by donating their free electron pairs [6]. Hydrochloric acid (HCl) is widely used as pickling solution. Corrosion inhibitors are needed to reduce the corrosion rates of metallic materials in HCl pickling solution [7]. There are some reports about the pickling of magnesium by hydrochloric acid solutions in Refs. [8−10]. Therefore it is important to find the effective corrosion inhibitors for Mg in HCl solution.

From Refs. [11−15], it is understood that most of the research is focused on corrosion inhibitors for Mg alloys especially in aqueous and neutral organic solvents. However, the reports about the corrosion inhibition of Mg and its alloys in acidic media are very scanty [16]. Hence, the present investigation is carried out to study the effect of **(**4Z)-4-(3-Phenyl allylidene amino)-3-hydroxy naphthalene-1-sulfonic acid on corrosion inhibition of AZ31 Mg alloy in 0.05 mol/L HCl solution.

2 Experimental

2.1 Synthesis of (4Z)-4-(3-phenyl allylidene amino)-3-hydroxy naphthalene-1- sulfonic acid

All the chemicals used were of analar grade 1-amino-2-naphthol 4-sulphonic acid and cinnamaldehyde were mixed together in an erlenmeyer flask. The mixture was kept under microwave radiation for 4 min on the "M-high" setting and the product obtained was brownish in nature. The resulting solution was evaporated to remove the solvent. The product was washed several times and recrystallized from ethanol. Thin layer chromatography was used to check the purity of the compound. The yield obtained was about 84%. The chemical structure of the (4Z)-4-(3-phenyl allydene amino)-3-hydroxy naphthalene-1-sulfonic acid is shown in Fig. 1.

2.2 Elemental analysis

The Schiff base [(4Z)-4-(3-phenyl allydene amino)-3-hydroxy naphthalene-1-sulfonic acid] in this work was identified by many techniques. The elemental analysis (CHN) is listed in Table 1.

2.3 Spectral analysis

2.3.1 Electronic spectra

The electronic spectra of the ligand was recorded on DMSO on Pekin Elmer Lambde E2201 spectro photometer. The electronic absorption spectra of the ligand showed λ_{max} at 247 nm.

2.3.2 IR spectra

IR spectra was recorded on Perkin Elmer 783 spectrophotometer using KBr pellet. The characterized bands in the IR spectra are listed in the Table 2. The band in the region 1614 cm^{-1} is due to N═C, and bands in the region 1430 cm^{-1} and 3435 cm^{-1} are due to C═C and O—H, S═O gives bands at 1231cm^{-1} and S—O gives band at 650 cm^{-1} and C—N gives bands at 1384 cm^{-1}, respectively [18]. The infrared spectra are shown in Fig. 2.

2.4 Test materials

The material used in this study is AZ31 Mg alloy in the form of extruded condition and supplied in plates of 6 mm thickness. The chemical composition of the AZ31

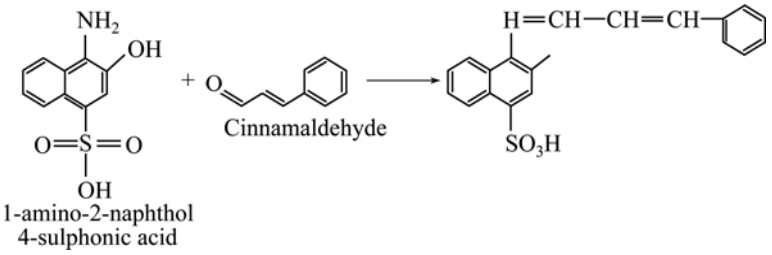

Fig. 1 Chemical structure of (4Z)-4-(3-phenyl allydene amino)-3-hydroxy naphthalene-1-sulfonic acid

Table 1 Elemental analysis data for CHN of Schiff base (4Z)-4-(3-phenyl allydene amino)-3-hydroxy naphthalene-1-sulfonic acid

Molar mass/ ($g \cdot mol^{-1}$)	Mole fraction/%					
	Calculated C	Found C	Calculated H	Found H	Calculated N	Found N
353	64.58	63.80	4.28	4.05	3.96	3.73

Table 2 Characterized band of IR spectra of Schiff base (4Z)-4-(3-phenyl allydene amino)-3-hydroxy naphthalene-1-sulfonic acid

Wavenumber/cm^{-1}					
N═C	C═C	O—H	S═O	S—O	C—N
1614	1430	3435	1231	650	1384

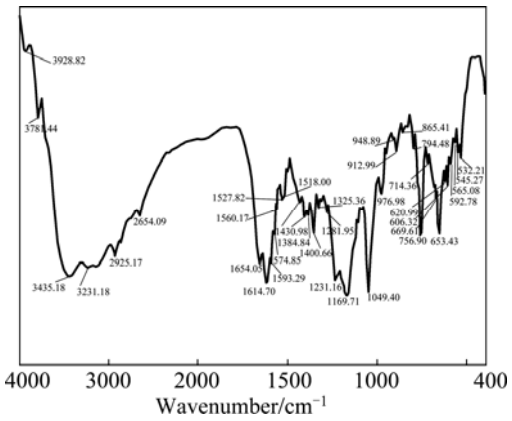

Fig. 2 IR spectrum of Schiff base (4Z)-4-(3-phenyl allydene amino)-3-hydroxy naphthalene-1-sulfonic acid

Mg alloy consists of 2.89% Al, 1.15% Zn, 0.2% Mn and the balance Mg. From the base metal AZ31 Mg alloy, the corrosion test specimens are sliced to the dimensions of 50 mm×16 mm×6 mm.

2.5 Mass loss method

Solution of HCl with concentration of 0.05 mol/L was prepared. For immersion corrosion testing, the test method consisted of immersing the specimens in an aquarium filled with HCl solution with and without inhibitor at room temperature as per ASTM G31. Prior to immersion, the Mg alloy specimens were polished with 4/0, 3/0, 2/0 and 1/0 grade emery papers, washed thoroughly with doubly distilled water, degreased with acetone and finally dried in air. The corrosion rate of the AZ31 Mg alloy specimen was estimated by mass loss measurement. The original mass (m_0) of the specimen was recorded before immersion and then the specimen was immersed in the solution of NaCl for immersion time of 24 h.

The corrosion products were removed by immersing the specimens for 1 min in a solution prepared by using 50 g chromium trioxide (CrO_3), 2.5 g silver nitrate ($AgNO_3$) and 5 g barium nitrate ($Ba(NO_3)_2$) for 250 mL distilled water. Finally, the specimens were washed with distilled water, dried and weighed again to obtain the final mass (m_1). The mass loss (Δm) can be measured using the relation as follows:

$$\Delta m=m_0-m_1 \quad (2)$$

where Δm is the mass loss; m_0 is the original mass before test; and m_1 is the final mass after test.

The corrosion rate (υ) of AZ31 was calculated by the equation as per the ASTM standards G31 as follows:

$$\upsilon=\frac{8.76\times10^4\times\Delta m}{A\times D\times t}\ \text{mm/a} \quad (3)$$

where A is the surface area of the specimen (cm^2); D is the density of the material (1.8 g/cm^3); t is the spraying time (h).

2.6 Electrochemical method

Electrochemical measurements were conducted using a Gamry AC potentiostat electrochemical workstation with a three-electrode cell arrangement at room temperature. AZ31 Mg alloy was used as a working electrode (WE), and a platinum wire was used as a counter electrode (CE). Testing electrolyte of 0.05 mol/L HCl acidic solution was prepared. All the reported potentials were referred to the saturated calomel electrode (SCE). The potentiodynamic polarization curves were obtained using a sweep rate of 2 mV/s in the potential range of ±2000 mV versus the open circuit potential. In the EIS experiments, the measured frequency range was 1−10 MHz at the open circuit potential by applying 10 mV sine wave AC voltage. All the measurements were repeated three times to check the reproducibility, and the impedance data were analyzed using the ZSimpWin 3.00 software (EG&G, USA).

From the mass loss and electrochemical measurements, the inhibition efficiency (η_m) and surface coverage (θ) were calculated for the various inhibitor concentrations using the formulae as follows [17]:

$$\eta_m=[(\Delta m_b-\Delta m_{inh})/\Delta m_b]\times100\% \quad (4)$$

$$\theta=(\Delta m_b-\Delta m_{inh})/\Delta m_b \quad (5)$$

where Δm_b is the mass loss without inhibitor (blank) (g); Δm_{inh} is the mass loss with inhibitor (g).

3 Results and discussion

3.1 Mass loss method

The average mass loss data obtained for the AZ31 Mg alloy specimen in triplicates for various concentrations of inhibitor [(4Z)-4-(3-phenyl allydene amino)-3-hydroxy naphthalene-1-sulfonic acid] are listed in Table 3. From the mass loss data which was obtained by performing the experiment in triplicate with the data variation of 0.5 mg, it is clear that the mass loss of Mg alloy specimens decreases with increasing the inhibitor concentration. Furthermore, it is found that the corrosion

Table 3 Inhibition efficiency of Schiff base AC for AZ31 Mg alloy in 0.05 mol/L HCl solution

Inhibitor concentration/ (mmol·L^{-1})	Mass loss/g	Corrosion rate/(mm·a^{-1})	Inhibitor efficiency/%	Degree of surface coverage
Blank	28.123	20.07	−	−
2.5	20.271	14.47	27.92	0.2792
5	16.823	12.02	40.12	0.4012
7.5	12.683	9.05	54.90	0.5490
10	10.462	7.46	62.79	0.6279

rate is linearly proportional to the mass loss. This means that the corrosion rate decreases with the increase in concentration of the inhibitors, as listed in Table 3.

The results indicate that the mass loss of Mg alloy sample decreases while compared with the absence of Schiff bases (inhibitor) because the Schiff base forms a preventive layer on the metal surface due to azomethine group (—CH═N—) and aromatic cycles of the Schiff bases.

Hence, for this inhibitor, the inhibition efficiency (IE) also increases with the increase of concentration. The inhibitor efficiency results from Table 3 show maximum inhibition efficiency (62%) is observed in 0.01 mol/L concentration of the inhibitor. The degrees of surface coverage (θ) for different concentrations of inhibitor have been evaluated from the mass loss method.

This is due to the following reason. For this inhibitor, the surface coverage increases with the increase of concentration and reaches a limiting value at a higher inhibitor concentration. Correlation between θ values and inhibition efficiency suggests that the inhibitive action is through adsorption. Nitrogen atoms in acidic solution imine group as well as in heteroaromatic ring can be protonated. Physical adsorption may take place due to the electrostatic interaction between protonated forms of Schiff bases and ($MgCl_2^-$) species. Coordinate bond formation between electron pairs of heteroaromatic ring and metal surface can take place. Chemisorption of Schiff bases occurs following deprotonisation step of the physically adsorbed protonated forms of Schiff bases due to interaction of their π orbitals with metal surface.

From these experimental and spectral evidences, it is clear that these Schiff base compounds act as good inhibitor. The results of this study confirm that whenever two or more hetero atoms or electro active groups are present, the inhibition nature of compound is enhanced. In the examined inhibitor, the presence of —CH═N— group has contributed for the higher inhibition efficiencies. The molecule gets adsorbed through the interaction of both —CH═N— group and Cl atom having three lone pairs of electrons with the metal surface. This interaction favours the adsorption and film formation on the surface. The molecule possesses aromatic groups which favour the adsorption on metal surface. Further the molecules are big enough and planar to block more surface area of the Mg alloy.

3.2 Potentiodynamic polarization method

Figure 3 shows the potentiodynamic polarization curves of AZ31 Mg alloy in 0.05 mol/L HCl in the presence and absence of various concentrations of AC Schiff base. As can be seen, both the anodic and cathodic currents decrease after the addition of the Schiff base to the corrosive solution. This result suggests that the addition of the AC Schiff base reduces anodic dissolution and also retards the hydrogen evolution reaction. The values of corrosion potential (φ_{corr}) in the absence and presence of inhibitor at different concentrations are listed in Table 4. It is clearly seen that the corrosion potential values are shifted to more positive values in the presence of AC.

Generally, if the displacement in φ_{corr} after the addition of inhibitor is bigger than 85 mV, the inhibitor can be classified a cathodic or anodic type; and if the displacement is less than 85 mV, the inhibitor can be considered mixed type [19,20]. In this study, the maximum displacement in φ_{corr} value is lower than 85 mV towards anodic region, which indicates that the AC acts as a mixed type inhibitor. Other electrochemical corrosion parameters such as cathodic and anodic Tafel slopes (B_c and B_a), polarization resistance (R_p) and corrosion current density (J_{corr}) are also obtained from polarization curves, as listed in Table 4. The values of anodic and cathodic Tafel slopes were calculated from the linear region of the polarization curves. There are no significant changes in the cathodic and anodic Tafel slopes after the addition of Schiff base compound. This means that the studied compound cannot change the mechanism of Mg dissolution or hydrogen evolution. The addition of Schiff base increases the polarization resistance of Mg in 0.05 mol/L HCl, and this leads to a reduction in corrosion current. These results show that the used compound acts as an effective inhibitor for Mg in the studied corrosive media. The inhibition efficiencies η were calculated as follows [21]:

Table 4 Polarization parameters for AZ31 Mg alloy in 0.05 mol/L HCl in absence and presence of AC Schiff base with different inhibitor concentrations

Inhibitor concentration/(mmol·L^{-1})	Polarization resistance R_p/(Ω·cm^2)	Anodic slope B_a/(mV·dec^{-1})	Cathodic slope B_c/(mV·dec^{-1})	J_{corr}/(μA·cm^{-2})	φ_{corr} (vs SCE)/V	Inhibitor efficiency/%
Blank	698.6	141	162	165.07	−1.686	−
2.5	981.5	128	122	97.30	−1.664	28.83
5	1206.4	150	136	90.40	−1.644	42.09
7.5	1481.6	145	119	67.44	−1.638	52.84
10	4424.1	146	124	23.17	−1.616	84.42

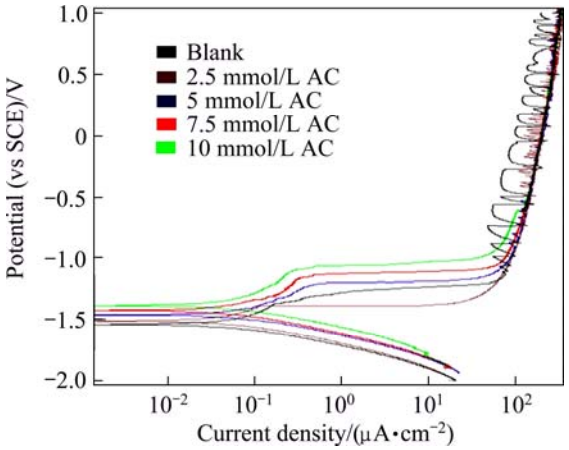

Fig. 3 Potentiodynamic polarization curves of AZ31 Mg alloy in 0.05 mol/L HCl in presence and absence of various concentrations of AC Schiff base

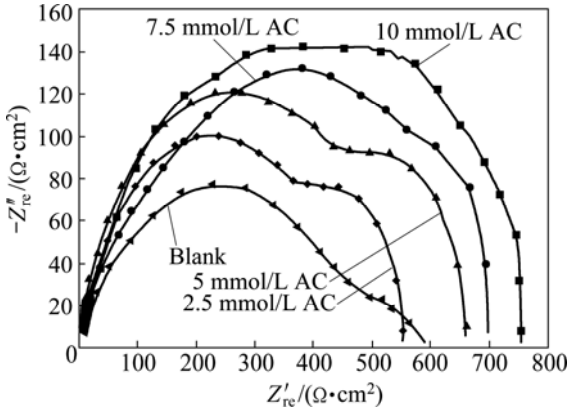

Fig. 4 Nyquist plots of AZ31 Mg alloy in 0.05 mol/L HCl solution in presence and absence of various concentrations of AC Schiff base

$$\eta=[(R_{inh}-R_{balnk})/R_{inh}]\times 100\% \quad (6)$$

The inhibitor efficiencies increase from 28.83% (lowest) to 84.42% (highest). Increasing inhibitor concentrations decreases corrosion current densities. The presence of inhibitors results in a slight shift of the corrosion potential towards the active direction in comparison to the result obtained in the absence of inhibitor. Both the anodic and cathodic current densities are decreased, indicating that the inhibitors suppress both of the anodic and cathodic reactions. This phenomenon may be due to the existence of a phenyl ring having high electron density. On the other hand, in the presence of inhibitors, both anodic and cathodic Tafel slopes almost remain unchanged, indicating that the inhibitors act by merely blocking the reaction sites of the metal surface without changing the anodic and cathodic reaction mechanisms.

3.3 Electrochemical impedance spectroscopy

The Nyquist plots of Mg in 0.05 mol/L HCl in the presence and absence of AC Schiff base compounds are shown in Fig. 4. The capacitive loop in the high frequency region (second semicircle) is always related to the charge transfer resistance (R_{ct}) and the double layer capacitance of the Mg surface [22,23]. From Fig. 4, it is obvious that the R_{ct} value in the corrosion potential is higher than that in the applied cathodic potential. A similar result in NaCl solution has been reported in Ref. [22]. Also, the presence of first capacitive loop at the highest frequencies is also observed. This capacitive loop arises from non-faradaic processes such as the adsorption of the hydrogen or chloride ions on Mg surfaces. Similar behavior has been observed for Mg or its alloys in alkali solutions [24]. Hence, during curve fitting, the first capacitive loop of the highest frequency is hidden for the better optimistic results. It is likely that the first capacitive loop at the highest frequencies is produced due to the adsorption of hydrogen ions. This matter calls for more mechanistic studies and is beyond the aim of the present investigation. It is found that the diameter of the capacitive semicircles, especially that of the second semicircle, increases with the increasing addition of the Schiff base. This effect is more obvious in the presence of high Schiff base concentrations. This result clearly demonstrates the high inhibition performance of AC Schiff base on Mg corrosion in acidic media.

The Nyquist plots are fitted to an appropriate equivalent circuit Fig. 5 and the relevant quantitative results are obtained. In this model, R_s, R_{ct} and R_f are the solution resistance, charge transfer resistance and partially protective film resistance, respectively, while the R_{ad} is inserted to account the resistance related with the first capacitive loop at the highest frequencies not shown in Fig. 5. Also, CPE_{dl} and CPE_f are used to model the capacitive behaviour of the electrical double layer and partially protective film, respectively. Moreover, the constant phase element CPE_{ad} is added to account for the capacitance of the first loop at the highest frequencies. In the used circuit, the constant phase elements (CPE) are used instead of the ideal capacitors because the Nyquist plots contain depressed semicircles with the center under the real axis. This is the characteristic behavior of solid electrodes. In such cases, it is necessary to use constant

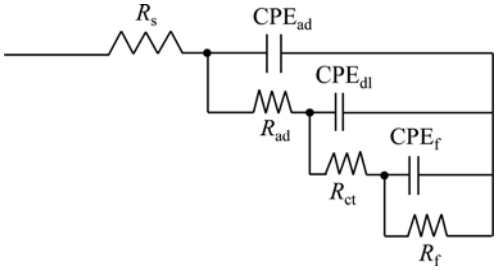

Fig. 5 Equivalent circuit for fitting EIS data

phase elements instead of the ideal capacitors to account for the non-ideal electrodes behavior. The constant phase elements impedance can be modelled as follows [20]:

$$Z_{CPE}=[j\omega C]^{-n} \quad (7)$$

where Z is the impedance; j is the square root of −1; ω is the angular frequency; C is the capacitance; and n is the measure of the non-ideality of the capacitor with a value in the range of $1>n>0$. It should be mentioned that the inductive loop elements are not entered in the circuits because the corresponding data are very scattered.

Therefore, the relevant data with low frequencies were not taken into account in the fitting process. The fitting was carried out using Zview2 software, and the produced data are listed in Table 5. The total resistance of the electrode surface is expressed as

$$R_{total}=R_{ad}+R_{ct}+R_f \quad (8)$$

The R_{total} is used to calculate the inhibition efficiencies (η) of the AC Schiff base of different concentrations based on the equation as follows:

$$\eta=[(R_{total}-R^0_{total})/R_{total}]\times 100\% \quad (9)$$

where R_{total} and R^0_{total} are the total resistances of Mg in the inhibited and uninhibited solutions, respectively. The calculated values are also listed in Table 5. As can be seen, the total resistance of the magnesium surface significantly increases after the addition of AC Schiff base, implying that the Schiff base compound acts as effective corrosion inhibitor for Mg in the studied corrosive solution.

Also as the inhibitor concentration increases, the inhibition efficiencies increase probably due to more AC molecules adsorbed on the Mg surface. For low inhibitor concentrations, the CPE_{dl} decreases as the inhibitor concentration increases. The decrease in CPE_{dl} is caused either by the reduction of the local dielectric constant and/or the increase of the electrical double layer thickness. This fact suggests that the studied inhibitor molecule acts by adsorption at the metal/solution interface [25]. The results obtained from EIS measurements are in good agreement with that obtained from both potentiodynamic polarization and mass loss measurements. Electrochemical impedance spectroscopy and polarization curve measurements were repeated several times and observed that they were highly reproducible.

3.4 Adsorption isotherm

Corrosion inhibition of AZ31 Mg alloy in 0.05 mol/L HCl solution by inhibitors can also be explained based on molecular adsorption. The adsorption process is influenced by the chemical structures of organic compounds, the distribution of charge in molecule, the nature and surface charge of metal and the type of aggressive media [26]. Basic information on the interaction between the inhibitors and the mild steel surface can be provided by the adsorption isotherms [27]. Totally, adsorption isotherms provide information about the interaction among the adsorbed molecules themselves and their interactions with the electrode surface [28].

In order to obtain a proper adsorption isotherm, Langmuir, Temkin, and Freundluich adsorption isotherms were tested. Langmuir adsorption isotherm, which is given in Eq. (10) [29], was found to be more suitable. These parameters were calculated based on the optimized concentration of above inhibitors against corrosion of mild steel as follows:

$$C/\theta=[(1/K_{ads})/C] \quad (10)$$

where C is the inhibitor concentration; K_{ads} is the adsorption equilibrium constant; and θ is the surface coverage. Straight lines were obtained when C/θ were plotted against C, as shown in Fig. 6. The linear relationships suggest that the adsorption of inhibitors obeys the Langmuir adsorption isotherm. The straight line has an intercept of $1/K$ as shown in Eq. (11) which can determine the relation of constant K with the standard free energy as

$$\Delta G_{ads}=-2.303RT\times\lg(55.5K_{ads}) \quad (11)$$

where 55.5 is the molar constant of water in the solution at temperature of 30 °C. The negative values of ΔG_{ads}

Table 5 Impedance parameters for AZ31 Mg alloy in 0.05 mol/L HCl in absence and presence of AC Schiff base at different inhibitor concentrations

Inhibitor concentration/ (mmol·L^{-1})	Added resistance R_{ad}/(Ω·cm^{-2})	CPE_{ad}/ (nF·cm^{-2})	Charge transfer resistance R_{ct}/ (Ω·cm^2)	CPE_{dl}/ (nF·cm^{-2})	Film resistance R_f /(Ω·cm^2)	CPE_f/ (nF·cm^{-2})	Total resistance R_p/(Ω·cm^2)	Inhibitor efficiency/%
Blank	210.6	0.614	262.3	0.613	84.21	7.96	557.11	−
2.5	242.5	0.362	327.1	0.574	153.6	6.214	723.2	22.96
5	284.1	0.211	474.5	0.444	274.2	4.321	1033.1	46.07
7.5	427.4	0.162	947.6	0.517	213.4	2.067	1588.4	64.92
10	531.6	0.103	4124.3	0.500	26.3	0.932	4682.2	88.10

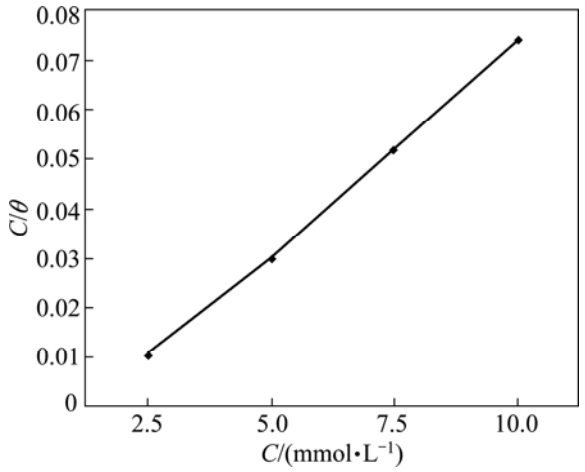

Fig. 6 Langmuirs adsorption isotherm plot based on EIS data

shown in Table 6 indicate that the adsorption of the inhibitors on the metal surface is spontaneous. Generally, the values of ΔG_{ads} around −20 kJ/mol or lower are consistent with the electrostatic interaction between the charged molecules and the charged metal surface (physisorption); those around −40 kJ/mol or higher involve charge sharing or transfer from organic molecules to the metal surface to form a coordinate type of metal bond (chemisorption) [30]. These values of ΔG_{ads} are less than 40 kJ/mol, which is commonly interpreted with the presence of physical adsorption by the formation of an adsorptive film with an electrostatic character [30,31].

Table 6 Adsorption parameters for AZ31 Mg alloy in 0.05 mmol/L HCl in absence and presence of AC Schiff base at different inhibitor concentrations

Inhibitor concentration/ (mmol·L^{-1})	Equilibrium constant, K_{ads}/(kJ·mol^{-1})	lg K_{ads}/ (kJ·mol^{-1})	ΔG_{ads}/(kJ·mol^{-1})
Blank	–	–	–
2.5	119.21	2.07	−22.162
5	170.85	2.23	−23.066
7.5	246.75	2.39	−23.995
10	740.33	2.86	−26.760

3.5 Mechanism of adsorption of Schiff bases compounds on metal surface

In the acidic solutions, Schiff bases exist either as neutral or in the protonated (cations) form. It is assumed that the Cl^- anion is first adsorbed onto the positively charged metal surface by columbic attraction. Then the protonated Schiff bases can be absorbed through electrostatic interactions between the positively charged molecules and the negatively charged metal surface [32].

The inhibitor [(4Z)-4-(3-phenyl allydene amino)-3-hydroxy naphthalene-1-sulfonic acid] contains three aromatic rings and a —CH═N— groups. The inhibitor may be adsorbed on the Mg surface through a combination of the following three probable adsorption mechanisms. 1) Protonation of nitrogen atoms of —CH═N— group could make the inhibitor molecule positively charged. The Mg surface gets negatively charged in NaCl solution. This could lead to an interaction that occurs between the positively charged inhibitor molecule and the negatively charged metal surface. 2) Unshared electron pairs on nitrogen atom could interact with the metal surface. 3) The flat orientation of the entire molecule with respect to the metal surface could lead to the interaction of π-electrons of the aromatic ring as well as —CH═N— groups with the metal surface.

4 Conclusions

1) The Schiff base AC shows an inhibiting effect on AZ31 Mg alloy corrosion in 0.05 mol/L HCl solution. From the mass loss measurements, it is showed that the inhibition efficiency increases with the increase of inhibitor concentration.

2) Potentiodynamic polarization curves show that Schiff base AC inhibits both anodic and cathodic reactions at all concentration, which indicate it is a mixed type inhibitor.

3) EIS results indicate that as the additive concentration increases, the polarization resistance increases whereas double-layer capacitance decreases.

4) The adsorption of Schiff base AC on the AZ31 Mg alloy surface in 0.05 mol/L HCl solution obeys the Langmuir adsorption isotherm.

5) The negative values of ΔG_{ads} reveal spontaneous adsorption of inhibitor on the metal surface and point to the physical nature of the adsorption on the Mg surface.

Acknowledgement

The authors are grateful to the Director, Dean, Principal and Managing Board of Sri Ramanujar Engineering College, Chennai for their encouragement and consistent support.

References

[1] HU J Y, HUANG D B, SONG G L, GUO X P. The synergistic inhibition effect of organic silicate and inorganic Zn salt on corrosion of Mg−10Gd−3Y magnesium alloy [J]. Corrosion Science, 2011, 53:

4093−4101.

[2] ZHANG J, CHAN Y F, YU Q S. Plasma interface engineered coating systems for magnesium alloys [J]. Progress in Organic Coatings, 2008, 61: 28−37.

[3] STANLEY C B, GEORGE L C, SCOTT J C. The separation of ketimine isomers [J]. Journal of American Chemical Society, 1963, 85: 26868−2869.

[4] MUNIR C, YOUSAF S M, AHMAD N. Synthesis, characterization and pharmacological properties of cobalt(II) complex of antibiotic ampicilin [J]. Journal of the Chemical Society of Pakistan, 1984, 7(4): 301−320.

[5] ASHASSI-SORKHABI H, SHAABANI B, SEIFZADEH D. Corrosion inhibition of mild steel by some schiff base compounds in hydrochloric acid [J]. Applied Surface Science, 2005, 239: 154−164.

[6] MIRGHASEM H, STIJN F L M, MOHAMMED G, MOHAMMED R A. Asymmetrical Schiff bases as inhibitors of mild steel corrosion in sulphuric acid media [J]. Materials Chemistry and Physics, 2003, 78: 800−814.

[7] ISSAADI S, DOUADI T, ZOUAOUI A, CHAFAA S, KHAN M A, BOUET G. Novel thiophene symmetrical Schiff base compounds as corrosion inhibitor for mild steel in acidic media [J]. Corrosion Science, 2011, 53: 1484−1488.

[8] HASSAN H E, KAZUHISA A, HIDETAKA K. Effect of surface pretreatment by acid pickling on the density of stannate conversion coatings formed on AZ91D magnesium alloy [J]. Surface and Coating Technology, 2007, 202: 532−537.

[9] SU H Y, LI W J, LIN C S. Effect of acid pickling pretreatment on the properties of cerium conversion coating on AZ31 magnesium alloy [J]. Journal of Electrochemical Society, 2012, 159(5): 219−225.

[10] HUANG Y H, LEE Y L, LIN C S. Acid pickling pretreatment and stannate conversion coating treatment of AZ91D magnesium alloy [J]. Journal of Electrochemical Society, 2011, 158(9): 310−317.

[11] HUANG D, HU J, SONG G L, GUO X. Inhibition effect of inorganic and organic inhibitors on the corrosion of Mg−10Gd−3Y−0.5Zr alloy in an ethylene glycol solution at ambient and elevated temperatures [J]. Electrochimica Acta, 2011, 56: 10166−10178.

[12] GAO H, LI Q, CHEN F N, DAI Y, LUO F, LI L Q. Study of the corrosion inhibition effect of sodium silicate on AZ91D magnesium alloy [J]. Corrosion Science, 2011, 53: 1401−1407.

[13] KARAVAIA O V, BASTOS A C, ZHELUDKEVICH M L, TARYBA M G, LAMAKA S V, FERREIRA M G S. Localized electrochemical study of corrosion inhibition in microdefects on coated AZ31 magnesium alloy [J]. Electrochimica Acta, 2010, 55: 5401−5406.

[14] GAO H, LI Q, DAI Y, LUO F, ZHANG H X. High efficiency corrosion inhibitor 8-hydroxyquinoline and its synergistic effect with sodium dodecylbenzenesulphonate on AZ91D magnesium alloy [J]. Corrosion Science, 2010, 52: 1603−1609.

[15] WILLIAMS G, MCMURRAY H N, GRACE R. Inhibition of magnesium localised corrosion in chloride containing electrolyte [J]. Electrochimica Acta, 2010, 55: 7824−7833.

[16] SEIFZADEH D, BASHARNAVAZ H, BEEZATPOUR A. A Schiff base compound as effective corrosion inhibitor for magnesium in acidic media [J]. Materials Chemistry and Physics, 2013, 88: 1−9.

[17] MOHAMMED Q M. Synthesis and characterization of new Schiff bases and evaluation as corrosion inhibitors [J]. Journal of Basrah Researches, 2011, 37(4): 116−130.

[18] ELISABETE A P, MARINA F M T. Determination of volatile corrosion inhibitors by capillary electrophoresis [J]. Journal of Chromatography A, 2004, 1051(1−2): 303−308.

[19] LI W, HE Q, ZHANG S, PEI C, HOU B. Some new triazole derivatives as inhibitors for mild steel corrosion in acidic medium [J]. Journal of Applied Electrochemisytry, 2008, 38(3): 289−295.

[20] VANESSA V T, ROBERTO S A, CAMILA F, TATIANA L F, CARLOS R, ALEXANDRE G T, ELIANE D. Inhibitory action of aqueous coffee ground extracts on the corrosion of carbon steel in HCl solution [J]. Corrosion Science, 2011, 53: 2385−2392.

[21] ASHASSI-SORKHABI H, SEIFZADEH D. Analysis of raw and trend removed EN data in time domain to evaluate corrosion inhibition effects of New Fuchsin dye on steel corrosion and comparison of results with EIS [J]. Journal of Applied Electrochemistry, 2008, 38(11): 1545−1552.

[22] SONG G, ATRENS A, JOHN D S, WU X, NAIRN J. The anodic dissolution of magnesium in chloride and sulphate solutions [J]. Corrosion Science, 1997, 39: 1981−2004.

[23] CAO C N. On the impedance plane displays for irreversible electrode reactions based on the stability conditions of the steady-state—II. Two state variables besides electrode potential [J]. Journal of Electrochimica Acta, 1990, 35: 837−844.

[24] ZIDOUNE M, GROSJEAN M H, ROUE L, HUOT J, SCHULZ R. Comparative study on the corrosion behavior of milled and unmilled magnesium by electrochemical impedance spectroscopy [J]. Corrosion Science, 2004, 46: 3041−3055.

[25] ASHASSI-SORKHABI H, SHAABANI B, SEIFZADEH D. Effect of some pyrimidinic Shciff bases on the corrosion of mild steel in hydrochloric acid solution [J]. Electrochimica Acta, 2005, 50: 3446−3452.

[26] MAAYTA A K, AL-RAWASHDEH N A F. Inhibition of acidic corrosion of pure aluminum by some organic compounds [J]. Corrosion Science, 2004, 46: 1129−1140.

[27] ISMAIL K M. Evaluation of cysteine as environmentally friendly corrosion inhibitor for copper in neutral and acidic chloride solutions [J]. Electrochimica Acta, 2007, 52: 7811−7819.

[28] NOOR E A, AL-MOUBARAKI A H. Thermodynamic study of metal corrosion and inhibitor adsorption processes in mild steel/ 1-methyl-4[4(-X)-styryl pyridinium iodides/hydrochloric acid systems [J]. Materials Chemistry and Physics, 2008, 110: 145−154.

[29] ABDALLAH M. Rhodanine azosulpha drugs as corrosion inhibitors for corrosion of 304 stainless steel in hydrochloric acid solution [J]. Corrosion Science, 2002, 44: 717−728.

[30] HOSSEINI S M A, SALARI M, GHASEMI M, ABASZADEH M. Enaminone compounds as corrosion inhibitors for austenitic stainless steel in sulphuric acid solution [J]. Journal Physical Chemistry, 2009, 223: 769−777.

[31] SOLMAZA R, KARDAS G, CULHA M, YAZICI B, ERBIL M. Investigation of adsorption and inhibitive effect of 2-mercaptothiazoline on corrosion of mild steel in hydrochloric acid media [J]. Electrochimica Acta, 2008, 53: 5941−5952.

[32] LAGRENEE M, MERNARI B, BOUANIS M, TRAISNEL M, BENTISS F. Study of the mechanism and inhibiting efficiency of 3,5-bis(4-methylthiophenyl)-4H-1,2,4-triazole on mild steel corrosion in acidic media [J]. Corrosion Science, 2002, 44: 573−588.

席夫碱作为缓蚀剂对盐酸溶液中 AZ31 镁合金的影响

S. THIRUGNANASELVI[1], S. KUTTIRANI[2], Amali Roseline EMELDA[1]

1. Department of Chemistry, Sri Ramanujar Engineering College, Chennai 600048, India;
2. Department of Chemistry, BS Abdur Rahman University, Chennai 600048, India

摘　要：在微波条件下，通过高纯度 1-氨基-2 萘酚 4-磺酸与肉桂醛的缩合反应制备席夫碱(4Z)-4-(3-苯基烯丙叉氨基)-3-羟基萘-1-磺酸(AC)。采用红外光谱对制备的席夫碱进行分析。研究席夫碱作为缓蚀剂对 AZ31 镁合金在 0.05 mol/L 盐酸中的缓蚀作用。通过质量损失法、动电位极化法和电化学交流阻抗谱(EIS)研究席夫碱化合物在 AZ31 镁合金腐蚀过程中的抑制作用。动电位极化曲线表明：席夫碱在所有浓度下能抑制阳极和阴极反应，是一种混合型缓蚀剂。EIS 结果表明：随着添加剂浓度的增加，极化电阻增加而双电层电容减少。在 0.05 mol/L 盐酸中，席夫碱 AC 对 AZ31 镁合金表面的吸附符合 Langmuir 吸附等温式。

关键词：席夫碱；AZ31 镁合金；缓蚀剂；动电位极化；电化学交流阻抗谱

(Edited by Chao WANG)